Aust. J. Phys., 1975, **28**, 543–55

The Use of X-ray Interferometry to Measure X-ray Refractive Indices

D. C. Creagh

Physics Department, Royal Military College, Duntroon, A.C.T. 2600.

Abstract

A Laue-case X-ray interferometer has been constructed to enable the measurement of X-ray refractive indices for X-ray wavelengths ranging from Ag $K\alpha_1$ to Fe $K\alpha_1$. Refractive indices have been measured for some alkali and alkaline-earth halides. From these the real part of the X-ray forward scattering amplitude $\Delta f_0'$ has been calculated for each atomic species. Comments are made on the validity of some of the assumptions made in quantum mechanical estimations of $\Delta f_0'$.

Introduction

Since the invention of Laue-case interferometers by Bonse and Hart (1965) a number of attempts have been made to determine the real part of the forward scattering amplitude $\Delta f_0'$ from measurements of the X-ray refractive index. The earliest experiment was that of Bonse and Hellkötter (1969) who measured the refractive indices of lucite, beryllium, lithium fluoride and sodium fluoride for Cu $K\alpha_1$ radiation. Their estimate of $\Delta f_0'$ for fluorine was more than twice the value calculated by Cromer (1965). At the same time Creagh and Hart (1970) measured the refractive index of lithium fluoride at wavelengths ranging from Ag $K\beta_1$ to Cu $K\alpha_1$. The values of $\Delta f_0'$ calculated from these measurements were in reasonably good agreement with Hönl's (1933*a*, 1933*b*) theory of anomalous dispersion. Bonse and Matterlik (1972) made measurements for nickel at the wavelength of Cu $K\alpha_1$, that is, on the long wavelength side of the K absorption edge. Their value for $\Delta f_0'$ was not in good agreement with Hönl's theory, and differed significantly from earlier measurements. Hart (1974) has since improved the accuracy of interferometer methods by using a variation of his (1968) Ångstrom ruler technique. He measured $\Delta f_0'$ for silicon at the wavelengths of Mo $K\alpha_1$ and Ag $K\alpha_1$. His values lie between those calculated by Wagenfeld *et al.* (1973) and those calculated by Cromer and Liberman (1970). It should be noted that all these authors found that $(\Delta f_0')_{Mo} - (\Delta f_0')_{Ag}$ is equal to 0·03. The present paper describes recent experiments using a Laue-case interferometer and discusses some of the problems encountered in the calculation of $\Delta f_0'$.

Experimental Techniques

Principles underlying the operation of an X-ray interferometer

Because a Laue-case interferometer consists of three spaced wafers machined from a large boule of single crystal silicon, it is an advantage to discuss the processes which occur when an X-ray beam passes through one of the crystal wafers. According to the dynamical theory of X-ray diffraction the propagation of electromagnetic

waves in a region, in which the electron density is a periodic function of position within the crystal, can be described by the simultaneous solution of Maxwell's equations and the Laue equation

$$\boldsymbol{K}_0+\boldsymbol{g} = \boldsymbol{K}_g, \tag{1}$$

where $\boldsymbol{K}_0$ and $\boldsymbol{K}_g$ are the wavevectors for the incident and diffracted waves, $\boldsymbol{g}$ is the reciprocal lattice vector for the effective Bragg reflection, and we have

$$|\boldsymbol{K}_0| = |\boldsymbol{K}_g| \quad \text{and} \quad |\boldsymbol{g}|^{-1} = d(hkl).$$

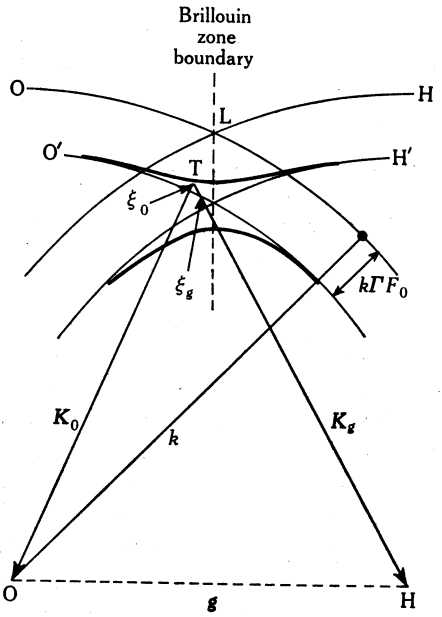

Fig. 1. Schematic representation of the dispersion surfaces (lower bold curve, branch 1; upper bold curve, branch 2) in the region of the Brillouin zone boundary (dashed line). $\boldsymbol{K}_0$ and $\boldsymbol{K}_g$ are the wavevectors of waves associated with the tiepoint T.

Within the Borrmann triangle, i.e. the volume enclosed by the direct and diffracted beams, there exists a standing wavefield whose properties are determined by the periodicity of the crystal lattice. The locus of all the wavevectors which are simultaneous solutions of Maxwell's equations and the Bragg equation is a family of surfaces called 'dispersion surfaces' (see Fig. 1). In the two-beam X-ray case these surfaces can be shown (see e.g. Batterman and Cole 1964) to form a pair of hyperbolic surfaces in the region of the Brillouin zone boundary (that plane which is normal to the midpoint of the reciprocal lattice vector $\boldsymbol{g}$). These surfaces have as asymptotes spheres centred at (000) and (hkl) in reciprocal space and having radii of $k(1-\Gamma F_0)$, where k is the vacuum wavevector, and ΓF_0 describes the effect of the average electron distribution on the wave velocity.

These hyperbolic surfaces can be described by the quantities ξ_0 and ξ_g which are respectively

$$\xi_0 = (\boldsymbol{K}_0 . \boldsymbol{K}_0)^{\frac{1}{2}} - k(1-\tfrac{1}{2}\Gamma F_0) \quad \text{and} \quad \xi_g = (\boldsymbol{K}_g . \boldsymbol{K}_g)^{\frac{1}{2}} - k(1-\tfrac{1}{2}\Gamma F_0).$$

The product

$$\xi_0 \xi_g = \tfrac{1}{4}k^2 P^2 \Gamma^2 F_g F_{-g}$$

is the equation of the hyperbolae, P is a factor which describes the polarization of

the incident beam, and F_g and F_{-g} are the geometrical structure factors for the reflections $\boldsymbol{g}$ and $-\boldsymbol{g}$ respectively. A point on one of the dispersion surface branches is referred to as a 'tiepoint'. These tiepoints describe the directional and absorptive properties of the waves and, as well, characterize the field amplitudes

$$D_g/D_0 = -2\xi_0/kP\Gamma F_{-g} = -kP\Gamma F_g/2\xi_g, \tag{2}$$

where D_g and D_0 are the complex field amplitudes associated with the X-ray polarization described by P. For points on the dispersion surface at the Brillouin zone boundary the ratio D_g/D_0 tends toward ± 1. The tiepoints that are active in a particular reflection depend on the orientation of the crystal surface with respect to the incident radiation, the orientation of the diffracting planes with respect to the crystal surface, and the divergence of the incident beam. X-ray interferometers are usually designed to operate in the symmetric Laue mode, i.e. the tiepoints excited by the incident radiation are symmetric about the Brillouin zone boundary.

For thick crystals, only those wavefields associated with the upper hyperbola (branch 2) persist because these wavefields have nodes at the atomic sites and therefore experience little photoelectric absorption. Wavefields associated with the lower hyperbola (branch 1) have their nodes between the atoms and their maxima at the atom sites. They therefore experience much more photoelectric absorption than the upper branch wavefields, and their field amplitude tends to zero with increasing crystal thickness. In this case, from equation (2) we have

$$D_{g1}/D_{01} = \xi_1 \approx 0 \qquad \text{and} \qquad D_{g2}/D_{02} = \xi_2 < 0.$$

The total wavefield has intensity

$$\begin{aligned} |D_2|^2 &= |D_{g2} + D_{02}|^2 \\ &= D_{02}^2 |1 + \xi_2^2 + 2\xi_2 \cos(2\pi \boldsymbol{r}.\boldsymbol{g})|. \end{aligned}$$

The survival of the wavefields associated with branch 2 of the dispersion surface was first observed by Borrmann (1941, 1950).

For thick crystals the beams which emerge from the crystal form a standing wavefield outside of the crystal surface, the antinodes of which lie between the atom planes. The crystal lattice has acted as a phase coherent beam splitter which has bent the rays through twice the Bragg angle.

In a thin crystal all the wavefields associated with branches 1 and 2 of the dispersion surface are present, and we have from equation (2)

$$D_{g1}/D_{01} = \xi_1 > 0 \qquad \text{and} \qquad D_{g2}/D_{02} = \xi_2 < 0.$$

In the symmetric Laue case we have

$$\xi_1 = \xi_2.$$

All the wavefields generated are phase coherent and the total field is given by

$$\begin{aligned} |D|^2 &= |D_{g1} + D_{01} + D_{g2} + D_{02}|^2 \\ &\propto 1 + \sin(2\pi \boldsymbol{g}.\boldsymbol{r}) \sin(2\pi \Delta^{-1}\tau), \end{aligned}$$

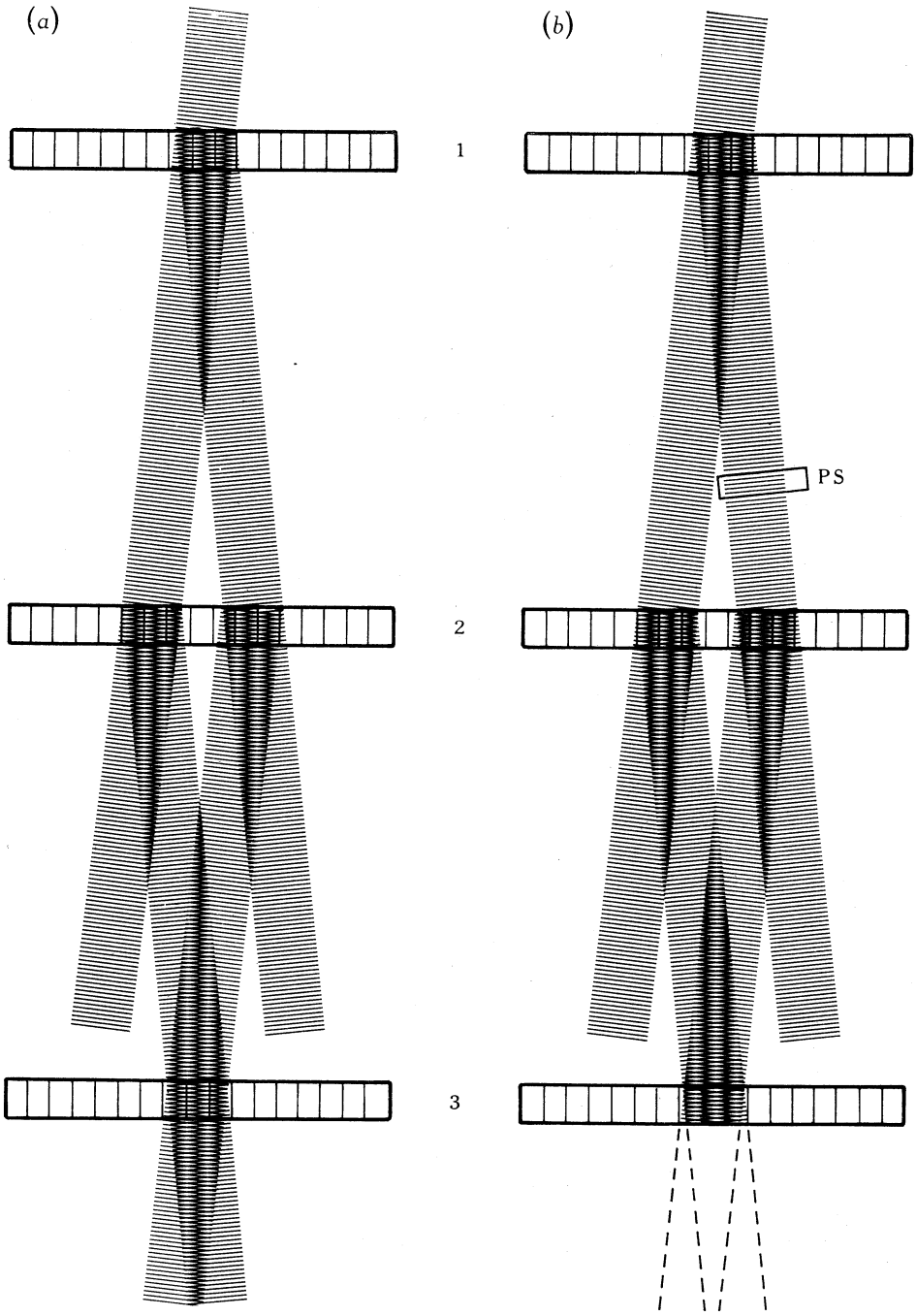

Fig. 2. Schematic representation of the wavefields present in an ideal interferometer. The wafers are labelled 1 to 3 and their Bragg planes are represented by vertical lines.

In case (*a*) the wavefields are present in the exit beams because the maxima of the standing wave patterns in front of wafer 3 lie in between the Bragg planes, and little photoelectric absorption occurs.

In case (*b*) a phase shifting object PS has been placed in one of the ray paths of the interferometer and has caused the standing wave pattern to coincide with the Bragg planes of wafer 3. The wavefields excited within the crystal experience severe photoelectric absorption and are rapidly attenuated.

where τ is the crystal thickness. This dependence of wavefield intensity on crystal thickness was predicted by Ewald (1958). The beams are still phase coherent but the intensity of the exit beam is a function of crystal thickness. If $\tau = p\Delta$ the wavefield is a maximum and the crystal behaves like an ideal mirror. If $\tau = (p+\frac{1}{2})\Delta$ the crystal again behaves like an ideal mirror. However, if $\tau = (p \pm \frac{1}{4})\Delta$ the beam is split into two parts, one in the incident beam direction, and the other in the diffracted beam direction. These beams have equal amplitudes and are phase coherent. Hence, careful choice of wafer thickness allows the incident beam to be divided into two phase coherent beams of equal amplitude (see Fig. 2). These beams can be recombined by subsequent interactions with other ideal beam splitters to form an interferometer.

In Laue-case interferometers the three wafers involved are produced by cutting into a single crystal boule. Sufficient material is left at the base of the wafers to ensure that the atomic planes of the wafers remain aligned with one another after machining. When an X-ray beam satisfies the Bragg condition in the first wafer, and if the wafer is of the correct thickness to behave like an ideal beam splitter, two beams leave the exit surface of the wafer and travel on to interact with the second wafer. Since the atomic planes in this wafer are aligned with the first wafer, the Bragg condition is satisfied and each incident beam is split into two beams, one travelling in the incident beam direction and the other in the diffracted beam direction. It is usual to make the thickness of the second wafer equal to that of the first. From the exit surface of this wafer, four phase coherent beams emerge. It is convenient to construct interferometers such that the distance between the first and second wafers is equal to the distance between the second and third wafers. In this case the two beams which converge after leaving the second wafer interact at the surface of the third wafer. Because they have a finite width they overlap in front of the third wafer and, being phase coherent, they interact with one another to form a standing wave pattern in front of the third wafer. The exact position of this standing wave pattern with respect to the atomic planes of the third wafer depends on the relative phases of the interacting waves. In the ideal interferometer just described, the maxima occur between the atomic planes and little absorption of the resultant waves results, so that the contrast is a maximum. However, if a difference in phases occurs, the maxima lie closer to the atomic planes and the waves encounter increased photoelectric absorption. The presence of phase shifting elements in the beam paths will therefore change the contrast in the outgoing beams. Furthermore, the third wafer transforms the atomic scale fringe pattern into a macroscopic pattern which can be observed using either film or counter techniques. The standing wavefield in front of the third wafer couples with the crystal lattice to form a moirè pattern. Inhomogeneous shifts in the beam paths will cause the standing wavefield to shift and the moirè pattern will change. It is this property of the interferometer which is used when X-ray refractive indices are measured.

Specimen mounting and preparation

The technique used in the measurement of refractive indices was the same as that described by Creagh and Hart (1970), and is shown schematically in Fig. 3. A thin plastic wedge was introduced into one beam path to produce a system of fringes in one of the exit beams. This fringe pattern is formed because the wedge rotates the standing wavefield in front of the final wafer, and the interaction of this

wavefield with the lattice causes a twist moirè pattern to be formed. The specimen crystal, which was a parallelopiped cleaved from a single crystal boule, was introduced into the other beam of the interferometer. Specimens of LiF and NaF have cleavage planes of the {100} type, and were mounted such that the (001) planes lay parallel to the X-ray beam. Specimens of CaF_2 were cleaved along {111} planes and were mounted such that these planes lay perpendicular to the X-ray beam. The insertion of the specimen caused a shift in the moirè fringe position because the refractive index of the specimen was different from that of air, and a phase advance of $2\pi(I+\varepsilon)$ ensued. Here I is an integer and ε is a fraction. The fringe pattern was recorded on Ilford L4 nuclear emulsion plates. These were developed using standard procedures (Meieran 1970) and the fringe positions were measured with a travelling microscope.

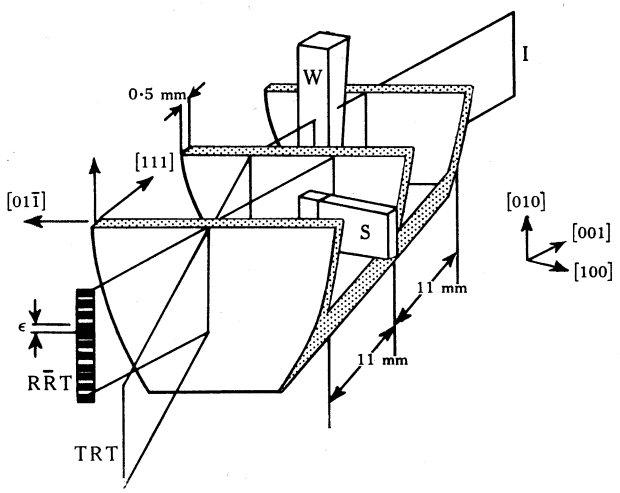

Fig. 3. Schematic representation of the use of an X-ray interferometer for the measurement of X-ray refractive indices. The symbols used are: I, incident X-ray beam; W, polyethylene wedge; S, specimen. Each wafer is 0·5 mm thick and the distance between wafers is 10·5 mm, while the useful surface area of the interferometer is about 10×10 mm^2.

The equipment on which the interferometer was mounted was placed in an enclosure to reduce the possibility of vibration of the wafers due to air currents. It was also necessary to mount the interferometer carefully on small balls of soft wax to prevent the transmission of externally generated vibrations to the interferometer. No special precautions were taken to control the temperature of the enclosure. The room which contains the X-ray equipment is air conditioned, and the temperature remained at 20° C throughout the duration of the experiments described in this paper. Sometimes the exposure times for the nuclear emulsion plates were long, approaching 48 h for experiments involving Fe $K\alpha_1$ radiation, although in most cases only 12 h exposure resulted in the production of acceptable contrast on the photographic plate.

The interferometer exhibited strong absorption at the longest wavelength used (Fe $K\alpha_1$) but only weak absorption at the shortest wavelength (Ag $K\beta$). In the latter case some pendellösung fringes occurred because of the interaction of the branch 1 and branch 2 wavefields in the interferometer wafers. However, these

fringes were of completely different character from the moirè fringes and their presence did not impair the accuracy to which the fractional fringe shift ε could be measured. Measurements of the fractional fringe shift were made for the characteristic radiations of silver, molybdenum, copper and iron. These were derived from Philips fine-focus X-ray tubes which were driven by a mains-stabilized Philips PW1120 generator.

All the specimens were tested for their crystalline perfection by diffracted beam X-ray topography using a camera described by Creagh (1972). Typically, dislocation densities were less than 10^4 cm^{-2}. The surfaces were free of cleavage steps. A Baker microscope fitted with a Cooke A.E.I. image splitting eyepiece was used to measure the specimen thickness. The error in the measurement of length was reduced to 0·001 mm using a statistical sampling technique.

Calculation of X-ray refractive indices

The change in fringe order p obtained when a specimen of thickness d is placed in one beam of the interferometer is given by

$$p = I+\varepsilon = (n-n_\alpha)d/\lambda,$$

where n is the refractive index of the sample, n_α is the refractive index of air $(1-1\cdot75\times10^{-9}\lambda^2)$ and λ is the X-ray wavelength. Experimentally, λ is known to better than 1 part in 10^5, d can be measured to 1 part in 500, and ε can be estimated to 0·02 of a fringe spacing. Using specimens of different thicknesses, one can measure I using Benoit's (1898) method of excess fractions. Hence the value of the specimen's refractive index can be determined to an accuracy of 0·2%.

Theory

When electromagnetic radiation passes through a region in which a distribution of charges exists it interacts with the charges and forces them to vibrate. This interaction causes a change in wave velocity relative to that in a region which does not contain a distribution of charges, and the medium is said to possess a refractive index n. This can be written as

$$n = 1-(\lambda^2/2\pi)r_e\rho f, \tag{3}$$

where λ is the X-ray wavelength, $r_e = e^2/4\pi\varepsilon_0 mc^2$ is the classical radius of the electron, ρ is the density of the charges and $f = f'+\mathrm{j}f''$ is the complex scattering power of the charge distribution. For a crystal the charge density can be written as the Fourier sum

$$\rho(\boldsymbol{V}) = V^{-1}\sum_{h,k,l} F_{hkl}\exp(-2\pi\mathrm{j}\,\boldsymbol{g}\cdot\boldsymbol{r}),$$

where F_{hkl} is the structure factor, $\boldsymbol{g} = h\boldsymbol{a}_1^*+k\boldsymbol{a}_2^*+l\boldsymbol{a}_3^*$ is the reciprocal lattice vector and V is the volume of the unit cell.

For the experiment discussed in this paper no active Bragg reflections occur, and measurements were made in the direction of the incident beam, which corresponded to values for (hkl) of (000). The quantity F_{000}/V represents the quantity ρf in equation (3). Like f, it is a complex number which is usually written as

$$F_{000}/V = \sum_a N_a(f_0+\Delta f_0'+\mathrm{j}\Delta f_0'')_a$$

for a system which contains N_a atoms of type a per unit volume. The value of $(f_0)_a$ corresponds closely to the atomic number of species a. The term $(\Delta f_0')_a$ is the real part of the dispersion correction and $(\Delta f_0'')_a$ is the imaginary part of the dispersion correction for atoms of type a. The latter term is always positive and corresponds to the scattering by the induced dipole which lags in phase by $\frac{1}{2}\pi$ relative to the primary wave. Since dipoles lying in any sheet parallel to the primary wavefront produce a resultant wave whose phase is retarded $\frac{1}{2}\pi$ behind the primary wave, the scattered wave corresponding to $(\Delta f_0'')_a$ lags by π. Consequently $(\Delta f_0'')_a$ adds a scattered wave component π out of phase with the primary wave, and the effect is therefore to diminish the amplitude of the primary wave, i.e. absorption occurs. However, the imaginary part does not affect the *phase* of the resultant wave. Measurements of refractive index based on the observation of phase shifts are related solely to the real part of the scattering factor.

Differences between methods of calculation of $\Delta f'$

All the calculations of the dispersion correction $\Delta f'$ have as their aim an estimation of the comparison between the scattering power of an electron bound into an orbital in a free atom and that of a completely free electron. The notions of classical electromagnetic theory were initially employed to calculate these scattering factors (see James 1948). The equivalence of the classical and quantum theory formulae was shown by James (1948) who used nonrelativistic perturbation theory, and by Cromer and Liberman (1970) who used Dirac–Slater wavefunctions in the development of their theory.

Classical Approach

Electromagnetic radiation traversing a region containing charges sets up an instantaneous polarization in the medium. Each electron behaves like an oscillating dipole and is therefore a source of radiation having the same frequency as the incident wave. Classical electromagnetic theory gives for the amplitude of a wave radiated in the equatorial plane by the dipole

$$A = \left(\frac{e^2}{8\pi\varepsilon_0 mc^2}\right)\left(\frac{\omega^2 E_0}{\omega_0^2-\omega^2+\mathrm{j}\delta\omega}\right),$$

where ω_0 is the natural frequency of the electron orbit, ω is the frequency of the incident wave and δ is the damping factor. The scattering power f is defined as the ratio of the amplitude scattered by the dipole to that scattered by a free electron. For an unbound electron, we have $\omega_0 = 0$ and $\delta = 0$, so that it follows that

$$f = \omega^2/(\omega^2-\omega_0^2-\mathrm{j}\delta\omega).$$

If measurements are not being made in the region of the absorption edge, the effect of the damping factor is not marked, and the scattering power of a dipole for which the resonant frequency is ω_s can be approximated by

$$f = f'+\mathrm{j}f'',$$

where

$$f' = \omega^2/(\omega^2-\omega_s^2) \quad \text{and} \quad f'' = \delta\omega^3/\{(\omega^2-\omega_s^2)^2+\delta^2\omega^2\}.$$

If a distribution of natural frequencies exists in the atom (taken for convenience to be a single-electron atom) and the probability of finding an electron with a natural frequency ω_s is $g(s)$, then the real part of the scattering factor becomes

$$f' = \sum_s g(s)\,\omega^2/(\omega^2-\omega_s^2),$$

which can be written as

$$f' = \sum_s g(s) - \sum_s g(s)\,\omega_s^2/(\omega_s^2-\omega^2).$$

Since we are considering the influence of the incident radiation on a one-electron atom, the first summation must be

$$\sum_s g(s) = 1,$$

which is the classical expression corresponding to the Thomas–Reiche–Kuhn sum rule in quantum mechanics. The second term is the dispersion correction $\Delta f_0'$ caused by the interaction between the single electron and the incident electromagnetic wave.

Transitions between virtual oscillator (bound) states can occur, but it can be shown that transitions to higher-level unoccupied states have a very small probability, and the only transitions which are significant correspond to transitions to positive (unbound) energy states. These transitions form a continuous set of values ranging from the binding energy of the electron upwards, so that the second summation becomes an integration. In the experiments performed on light atoms it is the interaction of the K-shell electrons that is important. If the lower frequency limit (given by the binding energy E_K of the K electrons) is ω_K, and if the number of virtual oscillators in the frequency range from ω to $\omega+\mathrm{d}\omega$ is given by $(\mathrm{d}g/\mathrm{d}\omega)\,\mathrm{d}\omega$, the total oscillator strength for the K electrons can be calculated to be

$$g_K = \int_{\omega_K}^{\infty} (\mathrm{d}g/\mathrm{d}\omega)_K\,\mathrm{d}\omega.$$

For a many-electron atom the effect of electrons of type k, for which the appropriate density of oscillator states is $(\mathrm{d}g/\mathrm{d}\omega)_k$ and the binding energy is $\hbar\omega_k$, becomes compounded by simple addition to give a formula for the total scattering power of the atom. Hence the formula for the real part of the scattering factor is

$$f' = f_0 + \Delta f_0',$$

where

$$\Delta f_0' = \sum_k \int_{\omega_k}^{\infty} \left(\frac{\omega^2(\mathrm{d}g/\mathrm{d}\omega)_k}{\omega_i^2-\omega^2}\right) \mathrm{d}\omega, \tag{4}$$

and f_0 is the scattering power at frequencies which are high compared with the natural frequencies of the atom. For many practical purposes f_0 is equal to Z, the total number of electrons in the atom. The expression (4) for $\Delta f_0'$ is the form into which all authors put their equations prior to computation. This expression should be compared with equation (26) of Cromer and Liberman (1970) and equation (3·42) of James (1948).

Methods of estimating $\Delta f_0'$

Three apparently different methods of estimating $\Delta f_0'$ have been given. Hönl (1933*a*, 1933*b*) used an approximation to the one-electron density of states for the K oscillator continuum calculated by Suguira (1927) on the assumption that the electrons had hydrogen-like wavefunctions. These early calculations have been extended by Barnea (1966) and Guttmann and Wagenfeld (1967). One of the problems with this type of computation arises from the fact that in formulating the wavefunctions a screening potential has to be used, and this causes an effective shift δ_k in the absorption edge to be used in the calculation. The influence of this approximation becomes more and more severe as the wavelength of the incident radiation approaches the wavelength of the absorption edge.

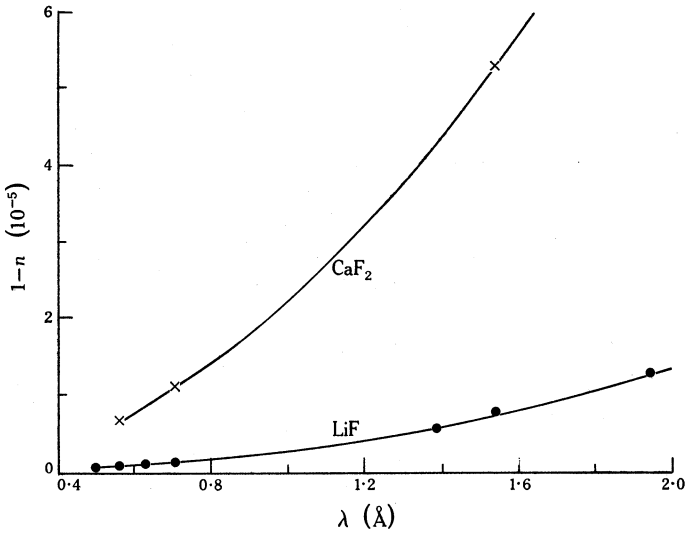

Fig. 4. Plot of measured X-ray refractive indices in the form $1-n$ as a function of the wavelength λ for LiF and CaF_2. The curves relate to values calculated using Hönl's (1933*a*, 1933*b*) theory.

Other theories are based on the semi-empirical theory of Parratt and Hempstead (1954). The approximation is made that the atomic absorption coefficient $\mu(\omega)$, which is directly proportional to the oscillator density of states, can be approximated by a power law of the form

$$\mu(\omega) = (\omega_k/\omega_i)^n \mu(\omega_k),$$

where $\mu(\omega_k)$ is the absorption coefficient at the absorption edge and n is a number which depends on the type of electron being considered. From this expression $\Delta f_0'$ can be calculated as

$$\Delta f_0' = \frac{2mc}{\pi e^2} \mu(\omega_k)\, \omega_k^n \int_{\omega_k}^{\infty} \frac{\omega^2}{(\omega_i^2 - \omega^2)\omega}\, \mathrm{d}\omega. \tag{5}$$

Cromer (1965) concluded that values of $\mu(\omega)$ were unreliable and attempted to calculate the $\mu(\omega_k)$ etc. from oscillator strengths. He recognized the deficiencies of this method, and subsequently Cromer and Liberman (1970) published a new set of

tables for the dispersion corrections based on the use of Dirac–Slater wavefunctions. They calculated the photoelectric cross section $\sigma(\hbar\omega)$ using the Brysk and Zerby (1968) program with data from Bearden (1967) as the eigenvalues for the wavefunctions. His value for $\Delta f_0'$ was put into the form

$$\Delta f_0' = \frac{mc}{2\pi^2\hbar e^2} P \int_{mc^2}^{\infty} \frac{(\varepsilon^+ - \varepsilon_1)^2 \sigma(\varepsilon^+ - \varepsilon_1)}{(\hbar\omega)^2 - (\varepsilon^+ - \varepsilon_1)^2} \, d\varepsilon^+ , \tag{6}$$

and suitable nonrelativistic approximations were made to eliminate some minor terms. In essence, however, all methods estimate $\Delta f_0'$ through the *photoelectric cross section*, which is either computed from measured *electronic energy level data* or from measured values of the *mass absorption coefficient*. Of the various attempts which have been made to estimate $\Delta f_0'$ and $\Delta f_0''$ the calculations of Cromer and Liberman (1970) have the soundest theoretical basis and were derived using the most rigorous set of computer programs developed to this time. Thus their results are often used as the standard with which the experimental values are compared.

Table 1. Comparison of experimental and theoretical values of $\Delta f_0'$

Source of results	$\Delta f_0'$ at the wavelength of Fe $K\alpha_1$ (1·93597 Å)	Cu $K\alpha_1$ (1·54051 Å)	Mo $K\alpha_1$ (0·70926 Å)	Ag $K\alpha_1$ (0·55936 Å)
		(*a*) *LiF*		
Present results	0·114±0·010	0·091±0·005	0·020±0·005	0·014±0·006
Cromer and Liberman (1970)	0·102	0·070	0·014	0·006
Hönl (1933*a*, 1933*b*)	0·106	0·073	0·020	0·014
		(*b*) *NaF*		
Present results		0·20 ±0·02	0·060±0·005	0·040±0·007
Cromer and Liberman (1970)		0·198	0·044	0·022
Hönl (1933*a*, 1933*b*)		0·202	0·061	0·042
		(*c*) CaF_2		
Present results		0·43 ±0·03	0·26 ±0·03	0·21 ±0·02
Cromer and Liberman (1970)		0·479	0·231	0·148
Hönl (1933*a*, 1933*b*)		0·43	0·257	0·207

Results

Measurements of X-ray refractive indices, using the methods described above, yield values which are accurate to ~0·2% because there are errors in the measurements of the phase shift of ~0·1% and the specimen thickness of ~0·1%. Typical results are shown in Fig. 4. The points plotted are for lithium fluoride and calcium fluoride for the wavelength range from Ag $K\beta$ to Fe $K\alpha$. The curves relate to values of refractive index calculated using Hönl's (1933*a*, 1933*b*) theory. When these results are processed to determine the real part of the dispersion correction the precision of the experiment decreases markedly because, although the error in the measured refractive index is small, when the molecular scattering factor f_0 is subtracted, the resulting value of $\Delta f_0'$ still has the same error as $f_0 + \Delta f_0'$.

The computed values of $\Delta f_0'$ are shown in Table 1 for the lithium fluoride, sodium fluoride and calcium fluoride molecules. These values are compared with the

theoretical predictions of Cromer and Liberman (1970) and the values obtained using Hönl's (1933*a*, 1933*b*) theory. Notice that there is a marked discrepancy between the experimental values and those computed by Cromer and Liberman. The measured values are always higher than their calculated values for lithium fluoride and sodium fluoride. For calcium fluoride the measured values are larger than the calculated values at the wavelengths Ag $K\alpha_1$ and Mo $K\alpha_1$, but less at Cu $K\alpha_1$. However, good agreement exists between the experimental values and those predicted using Hönl's theory.

D. T. Cromer (personal communication) has estimated the accuracy of his calculations of $\Delta f_0'$ to be within 2% of the value stated in his table. Because the values for $\sigma(\hbar\omega)$ predicted by Cromer and Liberman (1970) seem to be in reasonable agreement with experimental values (Creagh 1974), any error (if such exists) must lie either in the evaluation of the integral (6) or in the assumptions upon which the theory is based.

One of the likely sources of error is the assumption that the atoms involved are independent and essentially free of one another, a condition which is not fulfilled in practice. It could be argued that, because of the broadening of the energy levels in the formation of the solid, the density of oscillator states is altered, and the computed values of $\Delta f_0'$ are therefore in error. Aikala and Mansikka (1970, 1971) examined the effect that the crystal lattice has on the scattering factors of alkali halide molecules. They derived expressions for ionic crystals using free-ion wavefunctions. The nonorthogonality of these wavefunctions in the crystalline state was allowed for by the use of Lowdin's α-function technique (1956). The wavefunctions were derived by Clementi (1965) using the Hartree–Fock technique. Overlap between next and next-to-nearest neighbours was considered for the negative ions. Only next-neighbour overlap was considered for the positive ions. Calculations were performed for the alkali halides LiF, LiCl, LiBr, NaF, NaCl and KBr. In brief, they found that the static overlap contribution was small for large scattering angles. For moderate scattering angles the effect was quite marked, e.g. an increase in effective scattering factor of 0·10 electrons occurred for the 200 reflection from lithium fluoride ($f_0 = 7{\cdot}62$). Larger differences occurred for those alkali halides for which the overlap effect was more pronounced. In the forward direction, i.e. the direction of the X-ray beam, the effect was small, being $\sim$0·001 electrons. It may be concluded that, for the present experiment, the crystalline nature of the specimens has little effect on the scattering powers of the ions from which they are formed.

The discrepancy between the experimental results and the computed values of Cromer and Liberman (1970) cannot be explained by means of the perturbation of energy levels in the formation of free ions into a crystal. One must then examine the proposition that some systematic error has occurred in the evaluation of equation (6). Measurements of the mass absorption coefficients for alkali halide specimens have been performed by Creagh (1975). His values for the mass absorption coefficient are close to, but systematically larger than, the values quoted by Cromer and Liberman. It follows that, if these experimental values were inserted into equation (6), the resulting values of $\Delta f_0'$ would also be systematically larger than those of Cromer and Liberman.

The measured values tend to lie between those calculated by Cromer and Liberman (1970) and those calculated using Hönl's (1933*a*, 1933*b*) theory. In most cases the latter lie within the limits of error of the measured values. It can be concluded therefore that the scattering power of light elements is described more accurately

by the use of hydrogen-like wavefunctions than by the use of the more comprehensive relativistic Slater–Dirac wavefunctions.

The limitation of the photographic method to those atoms and wavelengths for which specimen absorption is small renders this method unsuitable for a definitive test between the theories of X-ray dispersion. A new method described by Hart (1974) shows promise of producing highly accurate (to 1% precision) measurements of $\Delta f_0'$. Preliminary measurements on a silicon specimen gave a value of $\Delta f_0'$ which was the arithmetic mean of the two theoretical values. This implies that for this atomic number neither theory provides a good description of the X-ray scattering process. Further measurements by Hart on other materials should enable a more complete theory to be formulated.

Acknowledgment

The author wishes to thank the Geology Department, Australian National University, for the use of their diamond saw to fabricate the interferometer.

References

Aikala, O., and Mansikka, K. (1970). *Phys. Kondens. Mater.* **11**, 243–54.
Aikala, O., and Mansikka, K. (1971). *Phys. Kondens. Mater.* **13**, 59–66.
Barnea, Z. (1966). *J. Phys. Soc. Jap.* **21**, 961–4.
Batterman, B. W., and Cole, H. (1964). *Rev. Mod. Phys.* **36**, 681–717.
Bearden, J. A. (1967). *Rev. Mod. Phys.* **31**, 78–124.
Benoit, J. R. (1898). *J. Phys.* **7**, 57–67.
Bonse, U., and Hart, M. (1965). *Z. Phys.* **188**, 154–64.
Bonse, U., and Hellkötter, H. (1969). *Z. Phys.* **223**, 345–52.
Bonse, U., and Matterlik, G. (1972). *Z. Phys.* **253**, 232–9.
Borrmann, G. (1941). *Z. Phys.* **42**, 157–62.
Borrmann, G. (1950). *Z. Phys.* **127**, 297–323.
Brysk, H., and Zerby, C. D. (1968). *Phys. Rev.* **171**, 292–9.
Clementi, E. (1965). *IBM J. Res. Develop.* **9**, 2–14.
Creagh, D. C. (1972). *J. Phys.* E **5**, 831.
Creagh, D. C. (1975). *J. Phys.* E (in press).
Creagh, D. C., and Hart, M. (1970). *Phys. Status. Solidi* **37**, 753–8.
Cromer, D. T. (1965). *Acta Crystallogr.* **18**, 17–23.
Cromer, D. T., and Liberman, D. (1970). *J. Chem. Phys.* **53**, 1891–8.
Ewald, P. P. (1958). *Acta. Crystallogr.* **11**, 888–91.
Guttmann, A. J., and Wagenfeld, H. (1967). *Acta. Crystallogr.* **22**, 334–8.
Hart, M. (1968). *J. Phys.* D **1**, 1405–8.
Hart, M. (1974). Proc. Int. Conf. on Anomolous Scattering, Madrid (in press).
Hönl, H. (1933*a*). *Z. Phys.* **84**, 1–16.
Hönl, H. (1933*b*). *Ann. Phys.* **18**, 625–55.
James, R. W. (1948). 'The Optical Principles of the Diffraction of X-rays' (Bell: London).
Lowdin, P. O. (1956). *Advan. Phys.* **5**, 1–16.
Meieran, E. S. (1970). *Seimens Rev.* **37**, 39–80.
Parratt, L. G., and Hempstead, C. F. (1954). *Phys. Rev.* **94**, 1593–1601.
Suguira, Y. (1927). *J. Phys. Radium* **8**, 113–19.
Wagenfeld, H., Kuhn, J., and Guttmann, A. J. (1973). Proc. 1st Conf. European Group of IUC, Bordeaux.

Manuscript received 11 March 1975